

ADAPTIVE COMPLEX CONTAGIONS AND THRESHOLD DYNAMICAL SYSTEMS

LEON CHANG, JEFFREY COCHRAN, HENNING S. MORTVEIT, SIDDHARTH RAVAL,
AND MATTHEW SCHROEDER

ABSTRACT. A broad range of nonlinear processes over networks are governed by threshold dynamics. So far, existing mathematical theory characterizing the behavior of such systems has largely been concerned with the case where the thresholds are *static*. In this paper we extend current theory of finite dynamical systems to cover *dynamic thresholds*. Three classes of parallel and sequential dynamic threshold systems are introduced and analyzed. Our main result, which is a complete characterization of their attractor structures, show that sequential systems may only have fixed points as limit sets whereas parallel systems may only have period orbits of size at most two as limit sets. The attractor states are characterized for general graphs and enumerated in the special case of paths and cycle graphs; a computational algorithm is outlined for determining the number of fixed points over a tree. We expect our results to be relevant for modeling a broad class of biological, behavioral and socio-technical systems where adaptive behavior is central.

Keywords: graph dynamical system; sequential dynamical system; dynamic threshold; complex contagion; discrete dynamics; adaptive behavior

1. INTRODUCTION

Many biological, social and technical systems can be described as *dynamical processes over graphs*. A specific example is the spread of influenza in a human population [6]. Here, the vertices of a graph are used to represent the individuals of the population with edges representing their contacts. Each vertex is assigned a *vertex state* that captures the particular individual's disease status and possibly other relevant factors such as behavioral or immunological characteristics. Based on the current state and the health status of the neighbors, a *vertex function* governs the evolution of this particular individual's health state with time. The application of the entire ensemble of vertex functions determines how the global disease dynamics of the population evolves with time. Similar examples include social & behavioral systems [8, 4, 3], spread of malware on wired & wireless networks [5], and gene prediction [9].

Threshold functions are widely used to capture the *local dynamics* of systems such as those above. In its basic form, a threshold function with threshold k is a Boolean function that returns the value 1 (or true) if k or more of its binary inputs are 1, and returns 0 (or false) otherwise. The prominent role of threshold functions in modeling and applications makes it desirable to have a solid understanding of their properties. Existing theoretical work (see, e.g., [2, 17, 10, 7]) has largely been concerned with

the case where each vertex threshold k is fixed. While this may be adequate in many situations, there are systems where the threshold values naturally change with time. Again, taking influenza as an example, the immune system typically receives a boost for the particular flu virus strain after a clinical episode, effectively increasing one's threshold value for falling sick. For addictive behaviors such as smoking, the threshold (related to peer-pressure, for example) for re-smoking after quitting may often be less than the initial threshold. For more complex diseases such as malaria, which involves acquired immunity, one may see both drops and rises in threshold values: increased immunity is developed upon exposure whereas a loss of immunity occurs through times of no exposure [18]. Using the framework of *graph dynamical systems* (GDS), see for example [16, 15, 17, 14, 13, 12], we introduce three classes of dynamic threshold function that target the three cases described above and other complex contagions (see, e.g. [4, 8]).

The three dynamic threshold functions we consider differ from standard threshold functions by allowing the threshold of each vertex to change when its state transitions from 0 to 1 or from 1 to 0. Specifically, for the *increasing* (resp. *decreasing*) threshold function the vertex threshold increases (resp. decreases) by 1 under the $0 \rightarrow 1$ (resp. $1 \rightarrow 0$) transition. The *mixed* threshold function combines the behaviors of the increasing and decreasing threshold functions.

Paper outline. In Section 2 we introduce necessary background and terminology for graph dynamical systems along with definitions for *increasing*, *decreasing* and *mixed* threshold graph dynamical systems (ET-GDS). Our main result is presented in Section 3 and states that increasing, decreasing and mixed threshold *sequential* graph dynamical systems only have fixed points as attractors. Moreover, for the synchronous case with increasing, decreasing and mixed threshold functions periodic orbits have length at most 2. Our approaches use several techniques. Most notably, the argument for the sequential mixed threshold case uses an extension of a potential function argument developed by Marathe et al in [2]. The parallel mixed threshold argument extends the classical proof by Goles and Olivos. Whereas their proof was developed for neural networks, we limit the statement of our main proof to the case where all edge weights are 1. However, our proof for the synchronous mixed threshold case is given for neural networks. We also prove that increasing and decreasing threshold systems are topologically conjugated both in the synchronous and asynchronous case, and we demonstrate that the six classes of dynamic threshold systems have a common set up fixed points. In light of this fact, our next class of results in Section 4 are on enumeration of this common set of fixed points. Specifically, we consider the path and circle graphs since these are building blocks of more general graphs. Here we also present scaling properties for the number of fixed points as a function of graph size. Our final result is an algorithm for determining the number fixed points for dynamic threshold GDS when the graph is a tree. We remark that the problem of enumerating and finding fixed points is, in general, NP-complete [1].

2. DEFINITIONS AND TERMINOLOGY

First, we define *sequential dynamical systems* (SDS) and *generalized cellular automata* (GCA) which are both special cases of *graph dynamical systems* (GDS). We

largely follow the notation in [15]. Let X be a simple *graph* on $|X| = n$ vertices and K a finite set. Associated to each vertex $v \in \{1, 2, \dots, n\}$ is a *vertex state* $x_v \in K$. We write $x = (x_1, \dots, x_n)$ for the *system state*. Next, we let $n[v]$ be the sequence of vertices contained in the 1-neighborhood of v ordered in increasing order with v included. Also, let $x[v]$ denote the restriction of the *system state* to $n[v]$. For each vertex v we have a *vertex function*

$$f_v: K^{d(v)+1} \longrightarrow K,$$

where $d(v)$ is the *degree* of v , and an X -*local function* $F_v: K^n \longrightarrow K^n$ given by

$$F_v(x) = (x_1, \dots, f_v(x[v]), \dots, x_n).$$

The vertex function f_v takes the state of vertex v and its neighbors at time t as input and computes the state for vertex v at time $t+1$. The choice for when to use vertex functions or X -local functions depends on the context; X -local functions are typically used for sequential systems since these functions can be composed. Some of the concepts above are illustrated in Figure 1.

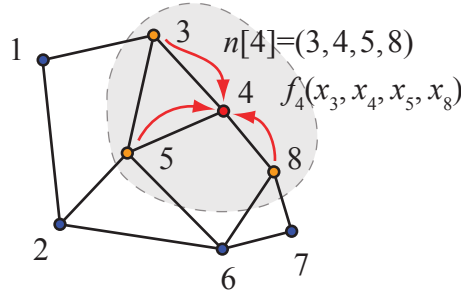


FIGURE 1. In the figure we have $n[4] = (3, 4, 5, 8)$, and $x[4] = (x_3, x_4, x_5, x_8)$. The vertex function f_4 takes $x[4]$ as input to compute the state of vertex 4 at the next time step.

Let S_X be the symmetric group over the vertex set of X . Here a permutation $\pi = (\pi_1, \dots, \pi_n) \in S_X$ induces an ordering $<_\pi$ on the vertex set by $\pi_k <_\pi \pi_l$ if and only if $k < l$, that is, $i <_\pi j$ if i occurs before j in π .

Definition 2.1 (SDS, GCA). Let $X, K, (f_v)_{v=1}^n$ and $\pi \in S_X$ be as above. The corresponding sequential dynamical system and generalized cellular automaton maps $\mathbf{F}_\pi, \mathbf{F}: K^n \longrightarrow K^n$ are defined by

$$\mathbf{F}_\pi = F_{\pi_n} \circ F_{\pi_{n-1}} \circ \dots \circ F_{\pi_1}$$

and

$$\mathbf{F}(x_1, \dots, x_n) = (f_1(x[1]), \dots, f_n(x[n])),$$

respectively.

Applying \mathbf{F}_π or \mathbf{F} to a system state $x \in K^n$ is called a *system update*, whereas applying F_v to x is called a *vertex update*. Here the GCA map \mathbf{F} corresponds to *synchronous/parallel* updating of vertex states, and the SDS map \mathbf{F}_π corresponds to *asynchronous/sequential* updating using the sequence π . The *phase space* of the

dynamical system with map $\phi: K^n \rightarrow K^n$ is the directed graph $\Gamma(\phi)$ with vertex set K^n and edge set $\{(x, \phi(x)) | x \in K^n\}$. A vertex or state on a cycle in $\Gamma(\phi)$ is a *periodic point* of ϕ ; a state on a cycle of length one is a *fixed point*. All other states are *transient states*. We denote the sets of periodic points and fixed points of ϕ by $\text{Per}(\phi)$ and $\text{Fix}(\phi)$, respectively. These points and their transitions represent the long-term behavior of the dynamical system ϕ .

In this paper we are concerned with generalizations of the case where the vertex functions are threshold functions. With state space $K = \{0, 1\}$, a *standard threshold function* $\tau_{k,m}: K^m \rightarrow K$ is defined by

$$\tau_{k,m}(x_1, \dots, x_m) = \begin{cases} 1, & \sigma(x_1, \dots, x_m) \geq k \\ 0, & \text{else,} \end{cases}$$

where $\sigma(x_1, \dots, x_m) = |\{i \mid x_i = 1\}|$. To each vertex v we associate a threshold value $k_v \in \mathbb{N}$. In contrast to standard threshold systems, we will not require that the thresholds k_v to be fixed, and will incorporate the vertex threshold in the vertex state. Thus, for each vertex v we have an *extended vertex state* $s_v = (x_v, k_v) \in K_v = \{0, 1\} \times D_v$ where $D_v = \{1, 2, \dots, d(v) + 1\}$. In our case, the system state is therefore an element of $\mathcal{S} = \prod_{i=1}^n K_i$. Note that we have excluded the constant functions (zero and one) through the choice of thresholds in the set D_v .

Definition 2.2. An extended threshold graph dynamical system (ET-GDS) is a GDS where each vertex function $f_v: \prod_{i \in n[v]} K_i \rightarrow K_v$ is given by

$$(1) \quad f_v(s[v]) = (\tau_{k_v, d(v)+1}(x[v]), g_v(x[v], k_v)),$$

where g_v is some function governing the evolution of the vertex threshold.

Although a slight abuse of terminology, we will occasionally call the tuple $x = (x_1, \dots, x_n)$ the *system state*, and the tuple of thresholds $k = (k_1, \dots, k_n)$ the *system threshold state* (k). Wherever the context warrants a distinction, we will refer to the tuple of extended vertex states $s = (s_1, \dots, s_n) = ((x_1, k_1), \dots, (x_n, k_n))$ as the *extended system state*.

In this paper, we consider three specific classes of ET-GDS corresponding to three choices of the function g_v in (1). For the *increasing threshold vertex function* the function g_v is given by

$$(2) \quad g_v^\uparrow(x[v], k_v) = \begin{cases} k_v + 1, & \text{if } x_v = 0 \wedge \sigma(x[v]) \geq k_v, \text{ and} \\ k_v, & \text{otherwise.} \end{cases}$$

Thus, for g_v^\uparrow the threshold k_v increases by 1 every time x_v transitions from 0 to 1. We denote the corresponding ET-SDS and ET-GCA by \mathbf{F}_π^\uparrow and \mathbf{F}^\uparrow .

Similarly, we define *decreasing ET-GDS* by letting the vertex threshold decrease by one whenever x_v is mapped from 1 to 0. We denote the corresponding maps by $g_v^\downarrow, f_v^\downarrow, F_\pi^\downarrow, \mathbf{F}_\pi^\downarrow$, and \mathbf{F}^\downarrow . Finally, a *mixed ET-GDS* combines the definitions of f^\uparrow and f^\downarrow . Specifically, the x_v component of the state is mapped as before using the function τ , whereas the threshold map g_v^\uparrow will increase (resp. decrease) k_v by 1 if $x_v = 0$ (resp. 1) and $\sigma(x[v]) \geq k_v$ (resp. $< k_v$), and will map k_v identically in the remaining case. For the mixed threshold function, the maps are denoted by $g^\uparrow, f^\uparrow, \mathbf{F}_v^\uparrow, \mathbf{F}_\pi^\uparrow$ and \mathbf{F}^\uparrow .

Example 2.3. Consider the case where the graph X is a 2-path with ET-GDS map \mathbf{F}_π^\uparrow and update sequence $\pi = (1, 2)$. The $(2^2)^2 = 16$ states and their transitions are shown in the phase space of $\Gamma(\mathbf{F}_\pi^\uparrow)$, see Fig. 2. Clearly, there are 10 fixed points and six transient states.

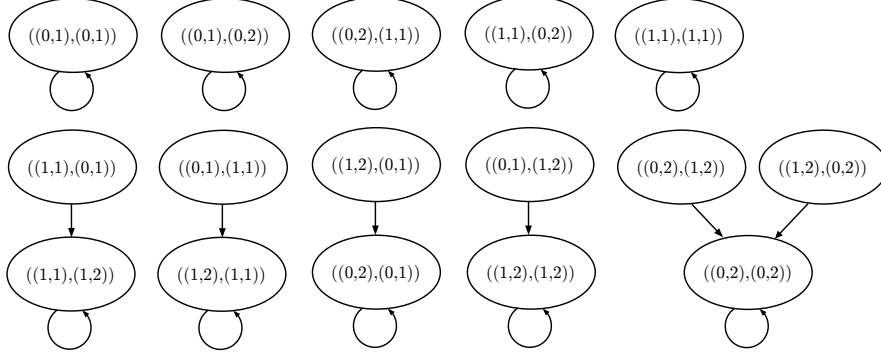


FIGURE 2. The phase space of Example 2.3. Each extended system state $s = ((x_1, k_1), (x_2, k_2))$ is outlined with an oval.

3. CHARACTERIZATIONS OF LIMIT SETS FOR ET-GDS

In this section we classify the periodic orbit structure of ET-GDS by proving the following result through a sequence of propositions and lemmas.

Theorem 3.1. *The maximal size of a periodic orbit for increasing, decreasing and mixed ET-SDS maps is 1. For ET-GCA maps, the maximal size is 2.*

Additionally, we relate the phase spaces of increasing and decreasing ET-GDS and show that their maps are topologically conjugated. We start by recalling the results for standard threshold systems. The proof of the statements in following lemma can be found in [2] for the sequential case and in [7] for the parallel case.

Lemma 3.2. *A standard threshold SDS (resp. GCA) map has no periodic orbit of size ≥ 2 (resp. ≥ 3).*

We can now state our result for increasing threshold GDS maps.

Proposition 3.3. *For any graph X and any update sequence $\pi \in S_X$ the ET-SDS map \mathbf{F}_π^\uparrow has no periodic orbit of length ≥ 2 . Similarly, the ET-GCA map \mathbf{F}^\uparrow has no periodic orbit of length ≥ 3 .*

Proof. Choose an arbitrary state $s = (x, k) \in \mathcal{S}$ and consider the orbit $\mathcal{O}(s)$ of \mathbf{F}_π^\uparrow starting at s . By definition, it follows that each component of k is non-decreasing and bounded along $\mathcal{O}(s)$. Since the state space is finite, there exists an integer $r \geq 0$ such that each k -component of $F_\pi^{\uparrow(u)}(s)$ is fixed for $u \geq r$. Consequently, for $u \geq r$ the dynamics of \mathbf{F}_π^\uparrow coincides with a standard threshold SDS over X , and, using Lemma 3.2, we conclude that s is eventually fixed. Since s was arbitrary, the

first statement follows. The proof for increasing threshold GCA maps is completely analogous and is therefore omitted. \square

A similar proof can be constructed for the decreasing threshold SDS and GCA, however a stronger statement is possible: increasing and decreasing threshold GDS maps are in fact topologically conjugated.

Proposition 3.4. *For any graph X and any update sequence $\pi \in S_X$ there exists a bijection $\psi: \mathcal{S} \rightarrow \mathcal{S}$ such that*

$$(3) \quad \psi \circ \mathbf{F}_\pi^\uparrow = \mathbf{F}_\pi^\downarrow \circ \psi ,$$

where $\mathcal{S} = \prod_i K_i$.

In other words, the maps \mathbf{F}_π^\uparrow and $\mathbf{F}_\pi^\downarrow$ are topologically conjugated. In other words, their phase spaces are isomorphic as directed graphs.

Proof. We prove this by constructing the bijection ψ in (3) directly. To this end, let $\psi = (\psi_1, \dots, \psi_n): \mathcal{S} \rightarrow \mathcal{S}$ be defined coordinate-wise by setting $\psi_i: \{0, 1\} \times D_i \rightarrow \{0, 1\} \times D_i$ equal to

$$(4) \quad \psi_i(x_i, k_i) = (x_i + 1 \bmod 2, d(v_i) - k_i + 2) .$$

We claim that ψ is its own inverse. To see this, let (x_i, k_i) denote an arbitrary vertex state for vertex i . Then

$$\begin{aligned} (\psi_i \circ \psi_i)(x_i, k_i) &= \psi_i(x_i + 1 \bmod 2, d(v_i) - k_i + 2) \\ &= ((x_i + 1) + 1 \bmod 2, d(v_i) - (d(v_i) - k_i + 2) + 2) = (x_i, k_i) , \end{aligned}$$

from which it follows that ψ is invertible and hence a bijection. To establish (3), we rewrite that equation as

$$\prod_i F_{\pi(i)}^\uparrow = \prod_i (\psi^{-1} \circ F_{\pi(i)}^\downarrow \circ \psi) .$$

Since $\psi^{-1} = \psi$ it is sufficient to establish that

$$(5) \quad \mathbf{F}_i^\uparrow = \psi \circ F_i^\downarrow \circ \psi$$

for each $i \in \{1, 2, \dots, n\}$. By the structure of the local maps and ψ , the conjugation relation clearly holds in all coordinates $j \neq i$ when we evaluate the two sides of (5) at a state s . This leaves three cases to consider:

Case 1: x_i is mapped from 0 to 1 by \mathbf{F}_i^\uparrow , which is possible only if $x_i = 0$, $\sigma(x[i]) \geq k_i$, and $(\mathbf{F}_i^\uparrow(s))_i = (1, k_i + 1)$. With $s' = \psi(s) = (x_j + 1 \bmod 2, d(v_j) - k_j + 2)_j$ we see that $x'_i = 1$, $k'_i = d(i) - k_i + 2$, and $\sigma(x'[i]) = d(i) - \sigma(x[i]) + 1 \leq d(i) - k_i + 1$. Therefore, $\sigma(x'[i]) \leq k'_i$ and \mathbf{F}_i^\downarrow maps s' to s'' where $x''_i = 0$ and $k''_i = d(i) - k_i + 1$. Then $\psi(s'')_i = (1, d(i) - (d(i) - k_i + 1) + 2) = (1, k_i + 1)$, establishing Case 1.

Case 2: x_i is mapped from 1 to 0 by \mathbf{F}_i^\uparrow . This case is similar to the first case. Here $x_i = 1$, $\sigma(x[i]) \leq k_i - 1$, and $(\mathbf{F}_i^\uparrow(s))_i = (0, k_i)$. Setting $s' = \psi(s) = (x_j + 1 \bmod 2, d(v_j) - k_j + 2)_j$, we see that $x'_i = 0$, $k'_i = d(i) - k_i + 2$, and $\sigma(x'[i]) = d(i) - \sigma(x[i]) + 1 \geq d(i) - k_i + 2 = k'_i$. Since $\sigma(x'[i]) \geq k'_i$ we see that \mathbf{F}_i^\downarrow maps s' to s'' where $x''_i = 1$ and $k''_i = k'_i = d(i) - k_i + 2$. Then $\psi(s'')_i = (0, d(i) - (d(i) - k_i + 2) + 2) = (0, k_i)$, establishing Case 2.

Case 3: x_i is mapped identically by \mathbf{F}_i^\uparrow . In this case we either have (i) $x_i = 1$ and $\sigma(x[i]) \geq k_i$ or (ii) $x_i = 0$ and $\sigma(x[i]) \leq k_i - 1$. In both cases we have $(\mathbf{F}_i^\uparrow(s))_i = (x_i, k_i)$ and $s' = \psi(s) = ((x_j + 1 \bmod 2, d(j) - k_j + 2))_j$. For case (i) $\sigma(x'[i]) = d(i) - \sigma(x[i]) + 1 \leq k'_i$, so with $s'' = \mathbf{F}_i^\downarrow(s')$ we have $x''_i = 0$ and $k''_i = d(i) - k_i + 2$. It follows that for this case $\psi(s'')_i = (1, k_i)$ as desired. Case (ii) is virtually identical with $\sigma(x'[i]) = d(i) - \sigma(x[i]) + 1 \geq d(i) - (k_i - 1) + 1 \geq k'_i$ leading to $x''_i = 1$ and $k''_i = d(i) - k_i + 2$ where $s'' = \mathbf{F}_i^\downarrow(s')$, and we have $\psi(s'')_i = (0, k_i)$ as required, concluding the proof for ET-SDS. \square

The argument in the proof combined with the structure of the map ψ ensure that (3) holds with \mathbf{F}_π^\uparrow and $\mathbf{F}_\pi^\downarrow$ replaced by \mathbf{F}^\uparrow and \mathbf{F}^\downarrow , respectively:

corollary 3.5. *For any graph X , the maps \mathbf{F}^\uparrow and \mathbf{F}^\downarrow are topologically conjugated.*

To conclude the proof of Theorem 3.1 we next turn to the case of mixed dynamic threshold SDS. The following result extends an earlier result in [2] for standard threshold systems.

Proposition 3.6. *The ET-SDS map \mathbf{F}_π^\uparrow has no periodic orbits of length ≥ 2 .*

Proof. Since individual threshold components (i.e., the k_i 's) are not necessarily monotone along orbits for \mathbf{F}_π^\uparrow , the previous arguments involving Lemma 3.2 cannot be put to use directly. Instead we use an extension of a potential function argument from [2].

Let X be a graph, $s = (x, k) \in \mathcal{S}$, $v \in v[X]$ and $e \in e[X]$. Also, let $T_1(s, v)$ denote the (dynamic) threshold value for vertex v (i.e., k_v), and let $T_0(s, v)$ denote the smallest number of states in $x[v]$ that must be zero to ensure that x_v is mapped to zero. Clearly, we have the relation $(d(v) + 1) - T_0(s, v) = T_1(s, v) - 1$, or $T_0(s, v) + T_1(s, v) = d(v) + 2$. We next introduce the vertex potentials

$$P(s, v) = \begin{cases} T_1(s, v), & x_v = 1 \\ T_0(s, v), & x_v = 0 \end{cases}$$

and the edge potentials

$$P(s, e = \{u, v\}) = \begin{cases} 1, & x_u \neq x_v \\ 0, & \text{otherwise,} \end{cases}$$

where $e = \{u, v\} \in e[X]$. The potential function $P: \mathcal{S} \rightarrow \mathbb{N}$ is defined as the sum of all vertex and edge potentials:

$$(6) \quad P(s) = \sum_{v \in v[X]} P(s, v) + \sum_{e \in e[X]} P(s, e)$$

Clearly, there exists positive integers m and M such that $m \leq P(s) \leq M$ for all $s \in \mathcal{S}$. Set $s' = \mathbf{F}_v^\uparrow(s)$.

Claim: *for each $s \in \mathcal{S}$ such that \mathbf{F}_v^\uparrow maps x_v non-identically we have $P(s') < P(s)$.* Clearly, any change in potential is solely associated with vertex v and edges incident with v . We write $n_0(s, v)$ and $n_1(s, v)$ for the number of neighbors of v with $x_v = 0$ and $x_v = 1$, respectively. There are two possible cases:

Case 1: If x_v is mapped from 0 to 1 then we have $n_1(s, v) \geq T_1(s, v)$, and, using the identity $T_0(v) + T_1(v) = d(v) + 2$ we get $n_0(s, v) \leq T_0(s, v) - 2$. Since $T_1(s', v) = T_1(s, v) + 1$ we obtain

$$\begin{aligned} P(s') - P(s) &= T_1(s', v) + n_0(s', v) - [T_0(s, v) + n_1(s, v)] \\ &\leq [T_1(s, v) + 1] + T_0(s, v) - 2 - T_0(s, v) - n_1(s, v) \leq -1. \end{aligned}$$

Case 2: When x_v is mapped from 1 to 0 we have $n_0(s, v) \geq T_0(s, v)$. This gives $n_1(s, v) \leq T_1(s, v) - 2$. We also have $T_0(s, v) + 1 = T_0(s', v)$ which yields

$$\begin{aligned} P(s') - P(s) &= T_0(s', v) + n_1(s', v) - [T_1(s, v) + n_0(s, v)] \\ &= T_0(s, v) + 1 + n_1(s, v) - T_1(s, v) - n_0(s, v) \\ &\leq n_0(s, v) + 1 + T_1(s, v) - 2 - T_1(s, v) - n_0(s, v) = -1, \end{aligned}$$

proving the claim. In light of the compositional structure of \mathbf{F}_π^\dagger and the boundedness of the potential function P , it follows immediately that \mathbf{F}_π^\dagger cannot have periodic orbits of length ≥ 2 since that would cause an immediate contradiction. This completes the proof of Proposition 3.6. \square

Remark 3.7. The particular choice of potential function used in the previous proof does not work directly for the synchronous case. To see this, consider the circle graph on four vertices with state $s = ((1, 2), (0, 2), (1, 2), (0, 2))$, which maps to $s' = ((0, 1), (1, 3), (0, 1), (1, 3))$, which in turn maps to s . Clearly, the edge potential is 4 for both states whereas the vertex potential of s and s' is 8 and 12, respectively.

The proof of Theorem 3.1 is completed by the following:

Proposition 3.8. *The ET-GCA map \mathbf{F}^\dagger has no periodic orbits of length ≥ 3 .*

Clearly, \mathbf{F}^\dagger may have fixed points. By the previous remark, we see that 2-cycles can occur for this class of maps.

Proof. This proof builds on a construction originally given by Goles & Olivos in [7] for neural networks and an extension of their proof that we developed in [10] that was needed to analyze the class of *bi-threshold* systems.

As in [7], we define the extended threshold function (neural networks)

$$(7) \quad \tau'_i(x_1, \dots, x_n) = \begin{cases} 1 & \text{if } x_i = 0 \text{ and } \sum_{j=1}^n a_{ij}x_j \geq k \\ 0 & \text{if } x_i = 1 \text{ and } \sum_{j=1}^n a_{ij}x_j < k \\ x_i & \text{otherwise,} \end{cases}$$

where $A = (a_{ij})_{ij}$ is a symmetric, real-valued matrix of dimension $n \times n$. Here $n = |v[X]|$. Our result, which we prove for τ' , will follow by specializing to the case where $a_{ij} = 1$ if $\{i, j\} \in e[X]$ and $a_{ij} = 0$ otherwise.

To start, let $s = (x, k) \in \mathcal{S}$ and assume that s reaches a periodic orbit of size T under \mathbf{F}^\dagger . We let $\{z(0), z(1), \dots, z(T-1)\}$ denote the sequence of (extended) states on this orbit, write z_i for the projection of this sequence onto its i^{th} component,

and let γ_i be the period of z_i . Clearly, γ_i must divide T . Let $Z = \{z_1, z_2, \dots, z_n\}$ and define the function $L: Z \times Z \rightarrow \mathbb{R}$ by

$$L(z_i, z_j) = a_{ij} \sum_{l=0}^{T-1} (x_j(l+1) - x_j(l-1))x_i(l),$$

with indices taken modulo T . Note again that the z_j s are extended system states. The operator L has the following properties (see [7, 10]):

- (i) $L(z_i, z_j) + L(z_j, z_i) = 0$ for $i, j \in \{1, \dots, n\}$ (anti-symmetry).
- (ii) If $\gamma_i \leq 2$ then $L(z_i, z_j) = 0$ for $j \in \{1, \dots, n\}$.

Let $z_i \in Z$ and suppose in the following that $\gamma_i \geq 3$. We set

$$\text{supp}(z_i) = \{l \in \{0, \dots, T-1\} : x_i(l) = 1\},$$

and write $\mathcal{I}(l) = \{l, l+2, l+4, \dots, l-4, l-2\}$. Next, set

$$C_0 = \begin{cases} \emptyset, & \text{if there is no } l_0 \in \{0, \dots, T-1\} \text{ such that } \mathcal{I}(l_0) \subset \text{supp}(z_i) \\ \mathcal{I}(l_0), & \text{otherwise.} \end{cases}$$

We define C_1 as the set

$$C_1 = \{l_1 + 2b \in \text{supp}(z_i) : b = 0, 1, \dots, q_1\},$$

where l_1 is the smallest index not in C_0 satisfying $x_i(l_1 - 2) = 0$ and q_1 satisfies $x_i(l_1 + 2q_1 + 2) = 0$. For $k \geq 2$ we define the sets C_k by

$$C_k = \{l_k + 2b \in \text{supp}(z_i) : b = 0, 1, \dots, q_k\},$$

where $l_k = l_{k-1} + r_k \pmod{T} \notin \{l_1, \dots, l_{k-1}\}$ is the smallest index for which $x_i(l_k - 2) = 0$ and q_k satisfies $x_i(l_k + 2q_k + 2) = 0$.

Since $\gamma_i \geq 3$ by assumption, there always exists $l_1 \in \text{supp}(z_i)$ for which $z_i(l_1 - 2) = 0$. This allows us to construct $\mathcal{C} = \{C_0, \dots, C_p\}$ which is a partition of $\text{supp}(z_i)$.

We will show that if $\gamma_i \geq 3$, then we are led to the conclusion that

$$\sum_{j=1}^n L(z_i, z_j) < 0.$$

As in [10], we can rewrite

$$\sum_{j=1}^n L(z_i, z_j) = \sum_{k=0}^p \Psi_{ik},$$

where

$$(8) \quad \Psi_{ik} = \sum_{j=1}^n a_{ij} \sum_{l \in C_k} (x_j(l+1) - x_j(l-1)).$$

If $C_0 = \emptyset$ then $\Psi_{i0} = 0$, and if $C_0 = \{l_0, l_0 + 2, \dots, l_0 - 2\}$ we have

$$\sum_{l \in C_0} (z_j(l+1) - z_j(l-1)) = 0.$$

In other words, we always have $\Psi_{i0} = 0$. Assume $k > 0$ in the following. From the assumption that $\gamma_i \geq 3$, there exists $C_k \neq \emptyset$ such that $C_k = \{l_k, l_k + 2, \dots, l_k + 2q_k\}$, so we can re-write Ψ_{ik} as

$$\begin{aligned}\Psi_{ik} &= \sum_{j=1}^n a_{ij} \sum_{s=0}^{q_k} (x_j(l_k + 2s + 1) - x_j(l_k + 2s - 1)) \\ &= \sum_{j=1}^n a_{ij} x_j(l_k + 2q_k + 1) - \sum_{j=1}^n a_{ij} x_j(l_k - 1).\end{aligned}$$

The dynamic threshold functions require that we distinguish the elements of \mathcal{C} more carefully than what was needed in [7]. An element $C \in \mathcal{C}$ is of *type ab* if $C = (l, l + 2, l + 4, \dots, k)$ and $x_{l-1} = a$ and $x_{k+1} = b$ where all indices are taken modulo T . Here we write $m_{ab} = m_{ab}(\mathcal{C})$ for the number of elements of \mathcal{C} of type *ab*. A key property needed here is that $m_{01} = m_{10}$. A proof of this fact is given in [10].

In the following four cases we assume that the threshold of vertex i at time $l_k - 2$ is k .

C_k **is of type 00**: in this case $x_i(l_k - 1) = 0$, $x_i(l_k) = 1$, $x_i(l_k + 2q_k + 1) = 0$ and $x_i(l_k + 2q_k + 2) = 0$, which is only possible if

$$\sum_{j=1}^n a_{ij} z_j(l_k - 1) \geq k \quad \text{and} \quad \sum_{j=1}^n a_{ij} z_j(l_k + 2q_k + 1) < k,$$

which implies that $\Psi_{ik} < 0$.

C_k **is of type 11**: this case is completely analogous to the 00 case, and

$$\sum_{j=1}^n a_{ij} x_j(l_k - 1) \geq k + 1 \quad \text{and} \quad \sum_{j=1}^n a_{ij} x_j(l_k + 2q_k + 1) < k + 1,$$

leading to $\Psi_{ik} < 0$.

C_k **is of type 10**: here $x_i(l_k - 1) = 1$, $x_i(l_k) = 1$, $x_i(l_k + 2q_k + 1) = 0$ and $x_i(l_k + 2q_k + 2) = 0$. This implies that

$$\sum_{j=1}^n a_{ij} x_j(l_k - 1) \geq k + 1 \quad \text{and} \quad \sum_{j=1}^n a_{ij} x_j(l_k + 2q_k + 1) < k,$$

so that $\Psi_{ik} < k - (k + 1) = -1$.

C_k **is of type 01**: this case is essentially the same as the 10 case, but here $\Psi_{ik} < k + 1 - k = 1$.

Using the above four cases, we now have

$$\sum_{j=0}^n L(z_i, z_j) = \sum_{k=0}^p \Psi_{ik} < 0 + m_{00} \cdot 0 + m_{11} \cdot 0 + m_{10}(-1) + m_{01}(+1) = 0,$$

where the last equality follows from the fact that $m_{10} = m_{01}$. As in the original proof, we see that the assumption $\gamma_i \geq 3$ leads to a contradiction since the sum of all terms $L(z_i, z_j)$ is zero by anti-symmetry. In effect, all the component periods γ_i for

$1 \leq i \leq n$ are bounded above by 2 which leads to the desired conclusion that $T \leq 2$. This also concludes the current proof as well as the proof of Theorem 3.1. \square

Increasing, decreasing and mixed ET-SDS also have a certain monotonicity property along orbits. We say that a state transition $(x, k) \mapsto (x', k')$ is *unidirectional* if all non-trivial transitions $x_v \mapsto x'_v$ with $x_v \neq x'_v$ are either all of the form (a) $0 \mapsto 1$ or (b) all of the form $1 \mapsto 0$. The following result is another extension of a result in [2] for standard threshold SDS maps to ET-SDS maps.

Proposition 3.9. *Let $\phi \in \{\mathbf{F}_\pi^\uparrow, \mathbf{F}_\pi^\downarrow, \mathbf{F}_\pi^\dagger\}$ and assume that for the state $s \in \mathcal{S}$ the transition $s \mapsto \phi(s)$ is unidirectional. Then all transitions along the forward orbit originating at s are also unidirectional and in the same direction as the one of $s \mapsto \phi(s)$.*

Proof. Let $\phi = \mathbf{F}_\pi^\dagger$, let $s, s', s'' \in \mathcal{S}$ and assume that $s \mapsto s'$ unidirectionally with all transitions going from 0 to 1. Assume next that $s' \mapsto s''$ but not unidirectionally, and let i denote the vertex minimal with respect to π for which 1 maps to 0 in the second transition. Since the previous transition was unidirectional ($0 \mapsto 1$), we must have $n_1(s, i) < n_1(s', i)$ at the time of the vertex update for i in the second transition. This yields a contradiction regardless of whether the threshold k_i was mapped to $k_i + 1$ or not in the first transition. The case where $s \mapsto s'$ unidirectionally with all transitions going from 1 to 0 is analogous. \square

4. STRUCTURE AND ENUMERATION OF FIXED POINT

This section is concerned with enumeration and characterization of fixed points of ET-GDS maps. Here we note that for a fixed sequence of vertex functions over a given graph X , the set of fixed points is the same whether we use a parallel or a permutation sequential update [17]. That is a general and well-known fact. We cover three graph classes: trees, the *path graph* P_n on n vertices (precursor for result on trees in next section), and the *circle graph* on n vertices denoted by C_n . However we first have the following result:

Proposition 4.1. *For any graph X and any $\pi \in S_X$ we have*

$$(9) \quad \text{Fix}(\mathbf{F}^\uparrow) = \text{Fix}(\mathbf{F}^\downarrow) = \text{Fix}(\mathbf{F}^\dagger) = \text{Fix}(\mathbf{F}_\pi^\uparrow) = \text{Fix}(\mathbf{F}_\pi^\downarrow) = \text{Fix}(\mathbf{F}_\pi^\dagger).$$

Proof. For a graph X , a sub-configuration $x[v]$ is a *local fixed point* if $f_v(x[v]) = x_v$. Two local fixed points ξ_i and ξ_j are *compatible* whenever they agree on the intersection $n[i] \cap n[j]$. Clearly, there is a bijective correspondence between the set of fixed points and the set of local fixed point sequences $\xi = (\xi_1, \dots, \xi_n)$ whose components are pairwise compatible. It is straightforward to see that for $f_i^\uparrow, f_i^\downarrow$ and f_i^\dagger to have ξ_i as a local fixed point, necessary and sufficient conditions are in all cases

$$(10) \quad (x_i = 0 \text{ and } \sigma(x[i]) < k_i) \quad \text{or} \quad (x_i = 1 \text{ and } \sigma(x[i]) \geq k_i),$$

and the proof follows. \square

Of course, the transient dynamics for these system classes will generally differ. The following result further characterizes the set $\text{Fix}(\mathbf{F}^\uparrow)$ appearing in (9).

Lemma 4.2. *For any graph X and any vertex $v \in v[X]$ we have $x_v = 1$ for precisely half of the elements of the set $\text{Fix}(\mathbf{F}^\uparrow)$.*

Proof. The map ψ in (4) induces a bijection $\psi' : \text{Fix}(\mathbf{F}^\uparrow) \rightarrow \text{Fix}(\mathbf{F}^\downarrow)$ by restriction. The result now follows from that that (i) $\text{Fix}(\mathbf{F}^\uparrow) = \text{Fix}(\mathbf{F}^\downarrow)$ and (ii) the image of any fixed point s for which $x_v = 1$ is a fixed point with $x_v = 0$ and vice versa. \square

A practical consequence of this results is that it can simplify fixed point enumeration.

4.1. Fixed Points of ET-GDS over P_n . In this section we enumerate the fixed points of dynamic threshold GDS over P_n . Both the result and its proof are relevant for the argument covering the case of trees in Section 4.3. Let Fib_n denote the n^{th} Fibonacci number ($\text{Fib}_0 = 0$, $\text{Fib}_1 = 1$ and $\text{Fib}_n = \text{Fib}_{n-1} + \text{Fib}_{n-2}$ for $n \geq 2$). We will also write $\text{Fib}(n)$ for Fib_n .

Proposition 4.3. *For $X = P_n$ we have $|\text{Fix}(\mathbf{F}^\uparrow)| = 2\text{Fib}_{3n-1}$.*

Proof. We proceed in a recursive manner constructing the fixed points over P_{n+1} from those over P_n . There are two disjoint sets of fixed points to consider: (i) the fixed points over P_{n+1} whose restrictions are fixed points over P_n , and (ii) their complement. Here we derive and solve a recursion relation where the second class of fixed points are charged to the first class. In this way, we can directly relate fixed points in the $(n+1)$ case to the n case and $(n-1)$ -case.

Clearly, the set of fixed points $s = (s_1, \dots, s_n)$ over P_n fall into six disjoint sets depending on the possible values for (s_{n-1}, s_n) which are $((0, *), (0, 1))$, $((0, *), (0, 2))$, $((0, *), (1, 1))$, $((1, *), (0, 2))$, $((1, *), (1, 1))$, and $((1, *), (1, 2))$ where $*$ denotes any element of $\{1, 2, 3\}$. Figure 3 shows the extended and charged fixed points in each of these six cases.

We set $\text{Fix}(n) = |\text{Fix}(\mathbf{F}^\uparrow)|$. Here, the two cases displayed on the last row in Figure 3 give rise to five fixed points. Each fixed point over P_{n-1} can be adjoined to precisely one of these cases, so the number of fixed points over P_{n+1} accounted for by these is $5\text{Fix}(n-1)$. Each of the remaining cases account for four fixed points and there are $\text{Fix}(n) - \text{Fix}(n-1)$ of these.

Direct computations give $\text{Fix}(2) = 10 = 2\text{Fib}_5$, $\text{Fix}(3) = 42 = 2\text{Fib}_8$ and $\text{Fix}(4) = 2\text{Fib}_{11}$. We proceed by induction and assume that the $\text{Fix}(n) = 2\text{Fib}_{3n-1}$ holds for $n \geq 4$. Then

$$\begin{aligned} \text{Fix}(n+1) &= 5\text{Fix}(n-1) + 4[\text{Fix}(n) - \text{Fix}(n-1)] \\ &= 5 \cdot 2\text{Fib}_{3n-4} + 4[2\text{Fib}_{3n-1} - 2\text{Fib}_{3n-4}] \\ &= 2\text{Fib}_{3(n+1)-1}, \end{aligned}$$

and we are done. \square

Scaling: It is known that Fib_n can be determined as the integer closest to $\varphi^n / \sqrt{5}$ where φ is the golden ratio. Thus, we see that the number of fixed points is roughly given by

$$(1 - 1/\sqrt{5})(\varphi^3)^n = (1 - 1/\sqrt{5})(2 + \sqrt{5})^n.$$

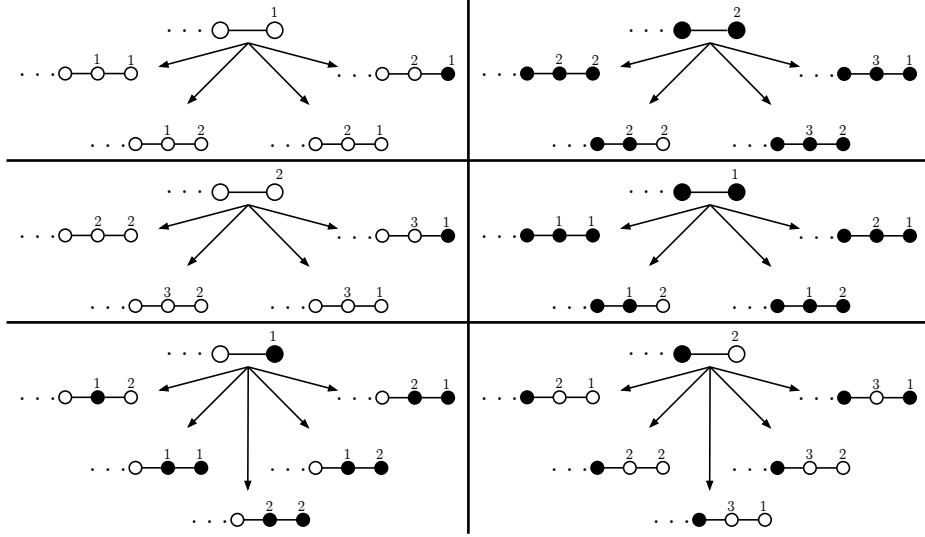


FIGURE 3. The extension & charging scheme used in the proof of Proposition 4.3. In the diagram, a filled (resp. empty) circle encodes a state that is 1 (resp. 0) while numbers give the threshold value.

For comparison, we note that for P_n there are $(4/9) \cdot 6^n$ states in phase space.

4.2. Fixed Points of ET-GDS over C_n . Specializing the proof of Proposition 4.1, we here derive a recursion relation for the number of fixed points for ET-SDS/ET-GCA over the graph C_n . Let Luc_n denote the n^{th} Lucas number ($\text{Luc}_0 = 2$, $\text{Luc}_1 = 1$ and $\text{Luc}_n = \text{Luc}_{n-1} + \text{Luc}_{n-2}$ for $n \geq 2$).

Proposition 4.4. *For $X = C_n$ we have $|\text{Fix}(\mathbf{F}^\dagger)| = 2 + \text{Luc}_{3n-1}$.*

Proof. The approach, which at its core is based on the matrix transfer method [19], patches the local fixed points to construct global fixed points, see [17, Chap. 5]. In the case of C_n , local fixed points are of the form

$$\xi_i = ((x_{i-1}, x_i, x_{i+1}), (k_{i-1}, k_i, k_{i+1})),$$

with indices taken modulo n . Such a tuple ξ_i is a local fixed point for \mathbf{F}_π^\dagger if $f_i^\dagger(\xi_i) = (x_i, k_i)$. Moreover, two local fixed points ξ_i and ξ_j are *compatible* whenever they agree on their intersection $n[i] \cap n[j]$ which is trivial unless i and j are ≤ 2 apart modulo n . We write $\xi_i \triangleleft \xi_{i+1}$ for compatible and consecutive local fixed points. Clearly, there is a bijective correspondence between the set of sequences of the form $\xi = (\xi_1, \dots, \xi_n)$ satisfying the conditions

$$\xi_1 \triangleleft \xi_2 \triangleleft \dots \triangleleft \xi_n \triangleleft \xi_1$$

and the set of fixed points of \mathbf{F}_π^\dagger over C_n . In the case of C_n there are 6 possible vertex states and $6^3 = 216$ tuples ξ_i , 144 of which are local fixed points. Extending the approach in [17, Chap. 5], we construct the adjacency matrix A for the graph G whose vertices are the local fixed points and with directed edges all $(\xi_i, \xi_{i'})$ such

that $\xi_i \triangleleft \xi_{i'}$. Using symbolic algebra software, it is straightforward to verify that the characteristic polynomial of A is

$$\chi_A(x) = x^{144} - 6x^{143} + 8x^{142} - 2x^{141} - x^{140} .$$

It follows that the number of fixed points L_n over C_n for \mathbf{F}_π^\uparrow satisfies the recursion relation

$$L_n = 6L_{n-1} + 8L_{n-2} - 2L_{n-3} - L_{n-4}$$

with initial values $L_3 = 78$, $L_4 = 324$, $L_5 = 1366$ and $L_6 = 5780$ obtained through direct calculations. This may be solved to give the explicit formula

$$(11) \quad L_n = 2 + (2 + \sqrt{5})^n + (2 - \sqrt{5})^n = 2 + \varphi^{3n} + (1 - \varphi)^{3n} = 2 + \text{Luc}_{3n} ,$$

completing the proof. \square

The simple form of (11) indicates that it may be possible to construct a proof similar to the one for the graph P_n in the previous section but instead using suitable extensions of fixed points over C_{n-1} and C_{n-2} .

Clearly, the number of fixed points scales with n as $(2 + \sqrt{5})^n$ whereas the number of total states in phase space is 6^n . We thus see that the number of fixed points over P_n and C_n essentially only differ by the constant factor $1 - \frac{1}{\sqrt{5}}$.

We remark that the method employed here for $ET - GDS$ and C_n can be extended to the graph $C_{n,r}$ where each vertex i is connected to all vertices j for which the graph distance in C_n is less than or equal to r ; this corresponds to the setting of radius- r elementary cellular automata. However, the book-keeping involved makes it somewhat impractical.

4.3. Fixed Points over Trees. In this section we describe an algorithm that can be used to determine the number of fixed points in (9) in the case where the graph X is a tree. The generalizations of this algorithm to general GDS maps over trees is being pursued elsewhere, so we only outline the ideas and illustrate with an example.

To avoid any confusion we will write T instead of X for the graph to emphasize this point when needed. The algorithm considers a tree as the *union of paths*, such that any two paths have at most one vertex in common. Recall that the *union* of two graphs X_1 and X_2 is the graph $X = X_1 \cup X_2$ with $v[X] = v[X_1] \cup v[X_2]$ and $e[X] = e[X_1] \cup e[X_2]$. Clearly, a tree T can be described as a union of paths p_i for which any pair of paths have at most one vertex in common. We denote the number of fixed points by $\text{Fix}(T)$, and for $v \in v[X]$ we write $\chi(v; X)$ for the number of fixed points over X with i^{th} component $s_i = (0, d_X(i) + 1)$. Here we use X as subscript in the degree $d_X(i)$ since i will appear as a vertex in multiple graphs.

As a specific example to illustrate the algorithm, we will consider the tree T shown in Figure 4. This tree has been split into paths p^* and p_1 through p_5 . The general idea is to first consider the graph consisting only of path p^* , and then find the fixed points as each additional path is appended in the order p_1, p_2, p_3, p_4 , and p_5 . We denote by T_1 the tree consisting of p^* and p_1 , by T_2 the tree T_1 with p_2 and so on. That is, we set $T_0 = p^*$ and $T_i = T_{i-1} \cup p_i$ for $1 \leq i \leq 5$. To compute the fixed points of T_i , we have to keep track of the vertices v_i where paths intersect.

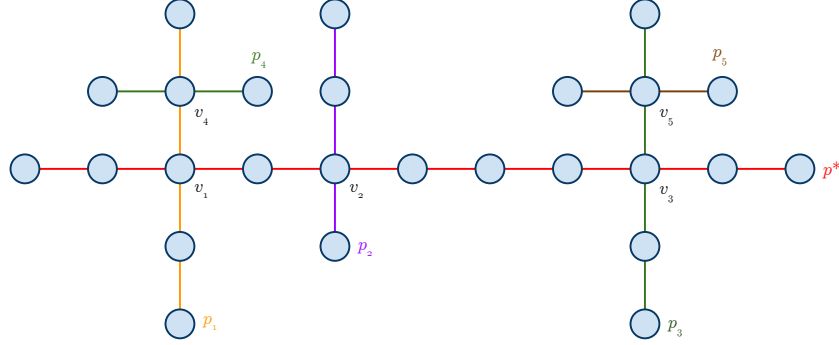


FIGURE 4. A tree illustrating the algorithm to determine $\text{Fix}(T)$ of Section 4.3.

The initial path p^* contains the three intersection vertices v_1 , v_2 , and v_3 . For each such vertex v_i , we need the number of fixed points of p^* where $s_i = (0, d_{p^*}(i) + 1)$ which is given by the following proposition.

Proposition 4.5. *Let p be a path on n vertices and denote by $r_i = r_i(p)$ the minimal distance (standard graph metric) of the vertex $v_i \in p$ to an end of p . Then we have*

$$(12) \quad \chi(p; v_i) = \text{Fib}(3(r_i + 1) - 2)\text{Fib}(3(n - r_i) - 2).$$

To keep track of the vertices v_2 and v_3 in trees T_i , we also need the number of fixed points of p^* where multiple vertices of intersection simultaneously satisfy $s_i = (0, d_{p^*}(i) + 1)$. For a set $\{v_\alpha\}$ of such vertices, we denote this quantity by $\chi(\{v_\alpha\}; p^*)$. Here we have:

Proposition 4.6. *Let $p = (V = \{v_1, \dots, v_n\}, \{e_1, \dots, e_{n-1}\})$ be a path, let $\{v_{\alpha_1}, \dots, v_{\alpha_m}\} \subset V$ with $\alpha_i < \alpha_{i+1}$, and split p into paths p_1, \dots, p_{m+1} . Then the number of fixed points over p where $s_{\alpha_i} = (0, d_p(\alpha_i) + 1)$ for all $1 \leq i \leq m$ is given by*

$$(13) \quad \chi(\{v_\alpha\}; p) = \chi(v_1; p_1)\chi(v_1; p_{m+1}) \prod_{i=1}^{m-1} \sum_{j=1}^{\alpha_{i+1} - \alpha_i} \text{Fib}(3j - 2).$$

With Propositions 4.5 and 4.6 in place we can now state the final result needed:

Theorem 4.7. *If $X = X_1 \cup X_2$, where X_1 and X_2 intersect in precisely one vertex v , then*

$$(14) \quad \text{Fix}(X) = \chi(v; X_1)\text{Fix}(X_2) + (\text{Fix}(X_1) - 2 \cdot \chi(v; X_1))\chi(v; X_2).$$

Using Theorem 4.7, we first compute $\text{Fix}(T_1)$ and proceed iteratively until we have arrived at the full tree T . For the first step we obtain

$$\begin{aligned}
\text{Fix}(T_1) &= \chi(v_1; p^*)\text{Fix}(p_1) + (\text{Fix}(p^*) - 2\chi(v_1; p^*))\chi(v_1; p_1) , \\
\chi(v_i, T_1) &= \chi(\{v_1, v_i\}, p^*)\text{Fix}(p_1) \\
&\quad + [\chi(v_i, p^*) - 2\chi(\{v_1, v_i\}, p^*)]\chi(v_1, p_1), \quad i = 2, 3 \\
\chi(\{v_2, v_3\}, T_1) &= \chi(\{v_1, v_2, v_3\}, T_1)\text{Fix}(p_1) \\
&\quad + [\chi(\{v_2, v_3\}, p^*) - 2\chi(\{v_1, v_2, v_3\}, p^*)]\chi(v_1, p_1) \\
\chi(v_4, T_1) &= \chi(v_1, p^*)\chi(v_1, p_1) + (\text{Fix}(p_1) - 2\chi(v_1, p^*))\chi(\{v_1, v_4\}, p_1) \\
\chi(\{v_i, v_4\}, T_1) &= \chi(\{v_1, v_i\}, p^*)\chi(v_4, p_1) \\
&\quad + [\chi(v_i, p^*) - 2\chi(\{v_1, v_i\}, p^*)]\chi(\{v_1, v_4\}, p_1), \quad i = 2, 3 \\
\chi(\{v_2, v_3, v_4\}, T_1) &= \chi(\{v_1, v_2, v_3\}, p^*)\chi(v_4, p_1) \\
&\quad + [\chi(\{v_2, v_3\}, p^*) - 2\chi(\{v_1, v_2, v_3\}, p^*)]\chi(\{v_1, v_4\}, p_1)
\end{aligned}$$

where each of the terms involving χ are computed using (12) and (13) where the factor $\chi(v_2; T_1)$ can be determined via Theorem 4.7, Lemma 4.2 and Proposition 4.6. In the same manner we get

$$\text{Fix}(T_i) = \chi(v_i; T_{i-1})\text{Fix}(p_i) + (\text{Fix}(T_{i-1}) - 2\chi(v_i; T_{i-1}))\chi(v_i; p_i) ,$$

for $2 \leq i \leq 5$. Careful evaluation shows that

$$\begin{aligned}
\text{Fix}(T_1) &= 1, 142, 003, 642, \\
\text{Fix}(T_2) &= 70, 046, 004, 938, \\
\text{Fix}(T_3) &= 18, 361, 190, 404, 154, \\
\chi(v_5, T_3) &= 4, 096, 066, 198, 731, \\
\text{Fix}(T_4) &= 263, 558, 770, 077, 330, \\
\chi(v_5, T_4) &= 58, 795, 434, 594, 819, \text{ and finally} \\
\text{Fix}(T) &= \text{Fix}(T_5) = 3, 783, 119, 360, 971, 626 .
\end{aligned}$$

Again, the details and generalizations of this algorithm with supporting proofs are being pursued elsewhere.

5. SUMMARY AND FUTURE WORK

In this paper we introduced *dynamic threshold* graph dynamical systems. This setting provides a more realistic model of phenomena involving complex contagions where the time evolution may affect the threshold values of the system entities. The results we have given on limit set structures and their enumeration may serve as a useful starting point for the development of mathematical models for such phenomena in a broad class of disciplines.

For application purposes, it is also desirable to know stability properties of the limit sets. Is a fixed point stable under a class of state perturbations? An example of such work is given in [11]. Shedding light on the stability of ET-GDS seems like a natural avenue for future work as does generalizations of the threshold models considered here. The potential function may be useful in this regard as it offers insight into the transient structure of the system. In particular, this could give

insight and bounds for convergence rates for dynamic threshold systems. From a combinatorial perspective, a more direct derivation of the recurrence relation enumerating fixed points over the circle graph through an extension/charging scheme would be desirable and may also shed some more light on the structure of the fixed points.

Finally, the assumption that the transitions where x_v switches from 0 to 1 and from 1 to 0 are governed by the common threshold k_v may not always be applicable. Work investigating dynamic threshold models with separate thresholds k_v -up and k_v -down is a natural extension of this work.

ACKNOWLEDGMENTS

We thank Samarth Swarup, Zhengzheng Pan, and Maleq Khan for discussions and valuable suggestions. Partial support for this work was provided through the NSF sponsored REU program “Modeling and Simulation in Systems Biology” at VBI, Virginia Tech 2010 (NSF Award Number: 0755322). We thank REU project PI and organizer Reinhard Laubenbacher for suggestions as well as for program coordination.

REFERENCES

- [1] Christopher Barrett, Harry Hunt, Madhav Marathe, S Ravi, Daniel Rosenkrantz, Richard Stearns, and Predrag Tosic. Garden of eden and fixed points in sequential dynamical systems. In *Discrete Mathematics and Theoretical Computer Science Proceedings*, pages 95–110, 2001.
- [2] Christopher L. Barrett, Harry B. Hunt III, Madhav V. Marathe, S. S. Ravi, Daniel J. Rosenkrantz, and Richard E. Stearns. Complexity of reachability problems for finite discrete sequential dynamical systems. *Journal of Computer and System Sciences*, 72:1317–1345, 2006.
- [3] Damon Centola. Failure in complex social networks. *Journal of Mathematical Sociology*, 33(1):64–68, 2009.
- [4] Damon Centola and Michael Macy. Complex contagions and the weakness of long ties. *American Journal of Sociology*, 113(3):702–734, November 2007.
- [5] K. Channakeshava, K. Bisset, M. Marathe, A. Vullikanti, and S. Yardi. High performance scalable and expressive modeling environment to study mobile malware in large dynamic networks. In *Proceedings of 25th IEEE International Parallel & Distributed Processing Symposium*, 2011.
- [6] Stephen Eubank, Hasan Glucu, V S Anil Kumar, Madhav V. Marathe, Aravind Srinivasan, Zoltan Toroczkal, and Nan Wang. Modeling disease outbreaks in realistic urban social networks. *Nature*, 429:180–184, May 2004.
- [7] E. Goles and J. Olivos. Periodic behavior in generalized threshold functions. *Discrete Mathematics*, 30:187–189, 1980.
- [8] Mark Granovetter. Threshold models of collective behavior. *American Journal of Sociology*, 83(6):1420–1443, May 1978.
- [9] Ulas Karaoz, T.M. Murali, Stan Letovsky, Yu Zheng, Chunming Ding, Charles R. Cantor, and Simon Kasif. Whole-genome annotation by using evidence integration in functional-linkage networks. *Proceedings of the National Academy of Sciences*, 101(9):2888–2893, 2004.
- [10] Chris Kuhlman, Henning S. Mortveit, David Murrugarra, and V. S. Anil Kumar. Bifurcations in Boolean networks. *Discrete Mathematics and Theoretical Computer Science*, AP:29–46, 2012. Automata 2011, 21–23 November, Santiago, Chile.
- [11] V. S. Anil Kumar, Matthew Macauley, and Henning S. Mortveit. Limit set reachability in asynchronous graph dynamical systems. In *Reachability Problems (RP) 2009*, volume 5797 of *Lecture Notes in Computer Science*, pages 217–232, Berlin/Heidelberg, 2009. Springer.
- [12] Reinhard Laubenbacher and Bodo Pareigis. Equivalence relations on finite dynamical systems. *Advances in Applied Mathematics*, 26:237–251, 2001.

- [13] Matthew Macauley, Jon McCammond, and Henning S. Mortveit. Dynamics groups of asynchronous cellular automata. *Journal of Algebraic Combinatorics*, 33(1):11–35, 2011. Preprint: math.DS/0808.1238.
- [14] Matthew Macauley and Henning S. Mortveit. Combinatorial characterizations of admissible coxeter sequences and their applications. Accepted 2011. Preprint: math.DS/0910.4376.
- [15] Matthew Macauley and Henning S. Mortveit. Cycle equivalence of graph dynamical systems. *Nonlinearity*, 22(2):421–436, 2009. math.DS/0709.0291.
- [16] H. S. Mortveit and C. M. Reidys. Discrete, sequential dynamical systems. *Discrete Mathematics*, 226:281–295, 2001.
- [17] Henning S. Mortveit and Christian Reidys. *An Introduction to Sequential Dynamical Systems*. Universitext. Springer Verlag, 2007.
- [18] T. Smith, N. Maire, A. Ross, M. Penny, N. Chitnis, A. Schapira, A. Studer, B. Genton, C. Lengeler, F. Tediosi, D. de Savigny, and M. Tanner. Towards a comprehensive simulation model of malaria epidemiology and control. *Parasitology*, 135:1507–1516, 2008.
- [19] Richard P. Stanley. *Enumerative Combinatorics: Volume 1*. Cambridge University Press, 2000.

DEPARTMENT OF APPLIED PHYSICS & APPLIED MATHEMATICS, COLUMBIA UNIVERSITY, LC2585@COLUMBIA.EDU

DEPARTMENT OF MATHEMATICS AND STATISTICS, GEORGETOWN UNIVERSITY, JDC62@GEORGETOWN.EDU

DEPARTMENT OF MATHEMATICS & NDSSL, VIRGINIA TECH, HMORTVEI@VBI.VT.EDU

DEPARTMENT OF MATHEMATICS, REED COLLEGE, RAVALS@REED.EDU

APPLIED MATHEMATICS, GENEVA COLLEGE, MATTHEW.SCHROEDER@GENEVA.EDU